Journal Pre-proof

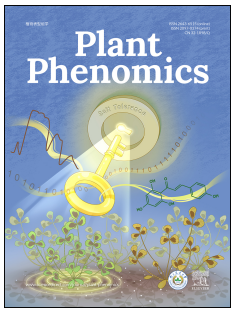

The Rapid Anatomics Tool (RAT): A low-cost root anatomical phenotyping platform reveals changes in root anatomy along the root axis

Dylan H. Jones, Juan C. Baca Cabrera, Dominik Behrend, Darren M. Wells, Joel F. Swift, Jonathan A. Atkinson, Maria Schön, Guillaume Lobet, Meredith T. Hanlon, Hannah M. Schneider

PII: S2643-6515(25)00156-6

DOI: https://doi.org/10.1016/j.plaphe.2025.100150

Reference: PLAPHE 100150

To appear in: *Plant Phenomics*

Received Date: 11 August 2025

Revised Date: 4 December 2025

Accepted Date: 17 December 2025

Please cite this article as: D.H. Jones, J.C. Baca Cabrera, D. Behrend, D.M. Wells, J.F. Swift, J.A. Atkinson, M. Schön, G. Lobet, M.T. Hanlon, H.M. Schneider, The Rapid Anatomics Tool (RAT): A low-cost root anatomical phenotyping platform reveals changes in root anatomy along the root axis, *Plant Phenomics*, https://doi.org/10.1016/j.plaphe.2025.100150.

SCIENCE PARTNER JOURNALS

Manuscript Template

FRONT MATTER

Title

The Rapid Anatomics Tool (RAT): A low-cost root anatomical phenotyping platform reveals changes in root anatomy along the root axis

Authors

Dylan H. Jones[1*], Juan C. Baca Cabrera[2], Dominik Behrend[3], Darren M. Wells[4], Joel F. Swift[5], Jonathan A. Atkinson[4], Maria Schön[1], Guillaume Lobet[2,6], Meredith T. Hanlon[7*], Hannah M. Schneider[1, 8*]

Affiliations

1: Leibniz Institute of Plant Genetics & Crop Plant Research (IPK) OT Gatersleben, Corrensstrasse 3, 06466 Seeland, Germany.

2: Institute of Bio- and Geoscience, Agrosphere (IBG-3), Forschungszentrum Jülich GmbH, Wilhelm-Johnen-Str., 52428 Juelich, Germany.

3: Institute of Crop Science and Resource Conservation (INRES) – Crop Science Group, University of Bonn, Katzenburgweg 5, 53115, Bonn, Germany.

4: School of Biosciences, University of Nottingham, Nottingham, United Kingdom.

5: Kansas Biological Survey and Center for Ecological Research, University of Kansas, Lawrence, Kansas, USA.

6: Earth and Life Institute, UCLouvain, 1348 Louvain-la-Neuve, Belgium.

7: Donald Danforth Plant Science Center, St Louis, Missouri, USA.

8: Division of Root Sciences, Department of Crop Science, Georg-August-University Goettingen, Goettingen, Germany.

Use a superscript asterisk (*) to identify the corresponding author and be sure to include that person's e-mail address.

The affiliation section should be followed by the statement:

Address correspondence to: m.hanlon@danforthcenter.org, schneiderh@ipk-gatersleben.de, jones@ipk-gatersleben.de

Abstract

Root anatomical phenotyping has become a demonstrably essential part of investigating root physiology and in acquiring a holistic understanding of plant development. However, accessible high throughput methods for root anatomical analysis are still lacking. Here, we present the Rapid Anatomics Tool (RAT), a novel, low-cost platform for high throughput root anatomical imaging with a shallow learning curve for obtaining high quality images suitable for comparative analysis across a number of plant species. Its efficiency comes from combining blockface-like imaging and stain-free imaging using near-ultraviolet (nUV) autofluorescence utilising a combination of low-cost commercial equipment, readily available mechanical components, and custom designed and 3D printed tools. Using this platform, we investigated the anatomy of mature tissue along the axis of wheat crown roots, revealing a tendency of reduction in vascular complexity (expressed through a reduction in metaxylem number, area, and mean area per metaxylem file) from the basal to the distal region of the root. This study highlights the importance of thorough sampling strategies for investigating root anatomy in relation to organ function and introduces an accessible, relatively high-throughput platform to support such research.

Keywords: anatomy, phenotyping, microscopy, 3D printing, root, wheat, xylem

INTRODUCTION

Importance of root anatomical phenotyping

Root anatomical phenotyping (typically; quantification of the presence, quantity, size, and distribution of different root cells and tissues) has become a mainstay of the integrated approaches used to investigate root functional traits, as well as in understanding development processes and evolutionary trajectories across a range of species and systems [1]. Phenotypic information of root anatomy can be used to understand radial and axial hydraulic conductance [2–4], nutrient capture [1,5], metabolic cost of root production and maintenance [6,7], the capacity for engagement with microbes and symbionts [8,9], and therefore environmental adaptation [10].

Root anatomical traits have a significant contribution to root physiology, affecting the movement of nutrients across the root from outside to within the root, and along the root, from the distal regions of the root system to the plant shoot. Even where anatomy is largely conserved in the arrangement of the major structural features, differences in the size, distribution, and cell wall properties of different tissues can significantly affect physiology. [11]. Several root anatomical traits have been shown to be under genetic control, including metaxylem area, stele size, and cortex size [12–16]. Many of the functional effects of different root anatomical traits in wheat have also been characterised in cereals. For example, enhanced drought tolerance is correlated with narrower vessels due to conservation of soil water through reduced transpiration [17,18]. Root cortical aerenchyma, which are air-filled lacunae in the cortex formed by programmed cell death, reduce the metabolic burden of the root tissue [19,20]. Because a root high in aerenchyma requires less carbon, N, and P for maintenance, these resources can be remobilized for greater root growth, which in turn facilitates more effective soil exploration and resource acquisition [21,22]. Another anatomical trait, fewer files of larger cortical cells, can also reduce metabolic costs and is associated with improved yields in water-limiting environments [23].

Historical Milestones

Root anatomy has been studied extensively over the course of history of modern science with interspecies differences in cell and tissue patterning in roots described in literature from the 17th century onwards [24,25]. In the early 20th century, the field of comparative anatomy was advanced significantly by Agnes Arber's thorough surveys focused on the anatomy of aquatic plants, monocotyledonous plants, and grasses [26]. This was followed by the publication in 1953 of Katherine Esau's 'Plant Anatomy' [27], still regarded as the definitive text in the field, and contemporarily, by the work of renowned botanist, cell biologist, and anatomist, Margaret McCully [28–32].

Several recent root anatomical studies in cereals have explored the associations between plant performance under varied environments and anatomical traits [7,33–35]. Using large germplasm panels not only enables observations of the functional properties of anatomical traits, but when integrated with genetic mapping enables association of anatomical traits with specific genes [1,12]. Root anatomical studies have also been used to understand environmental adaptation during domestication and evolution [36], as well as to investigate the range of functions of specific genes and molecular processes [14]. Significant opportunities remain to explore the precise quantitative impact of anatomical variation on root function under varied environmental conditions and to understand the complex genetic networks that govern these structural traits.

Current methods and limitations in anatomical phenotyping

Historically, progress in this area has been concentrated within a few research groups, a limitation imposed by a lack of accessible, high-throughput technology. In recent years, the call for a 'second green revolution' focused on the 'hidden half' [37,38] has driven an increase in exploration of root physiological traits for crop improvement. Rapid technological developments in recent decades have furnished researchers with a suite of new tools, albeit with a relatively low throughput, to investigate root physiology, capture phenotypic data on root anatomy, and relate this to functional properties, genetic mechanisms, and plant performance. The study of anatomy provides the essential scaffold for understanding biological function, yet to advance the field, we must move beyond simple qualitative observations and broad correlational relationships. For example, anatomical imaging can be integrated with modelling approaches to quantitatively explore how structural traits influence root function across genotypes or environmental conditions [39].

Being able to image roots at cellular resolution is a critical step in data collection and comparative analysis of root anatomy. Typically, this is done with light microscopy, requiring preparation of thin sections of plant tissue, followed by staining and microscope imaging, or alternatively, the use of highly specialized equipment employing visible light and other forms of radiation or particle detection in order to create a micrograph of plant cell structures. Though these techniques are powerful, versatile, and create enriched datasets alongside 2D anatomical images, brightfield microscopy remains the most common and accessible method of anatomical imaging available.

Despite the increasing availability and speed of digital imaging technologies, sample preparation, particularly the consistent production and handling of thin tissue sections, remains a major bottleneck in anatomical phenotyping workflows. Preparation of thin sections of tissue is essential for transmitted light microscopy, and desirable for confocal laser scanning microscopy, affecting light penetration, reflectance of out of plane light, dye penetration, background fluorescence, and sample topology. This requires at least two flat, consistent, and parallel cuts to be made in the sample, then for this delicate slice of tissue to be transferred to a staining solution and on to a slide without distortion.

A range of tools and techniques are available to prepare root cross-sections for anatomical analysis, each with specific trade-offs in costs (hardware and operating), throughput, versatility, and resolution. Traditional hand sectioning using razor blades or scalpels remains a common method due to its simplicity and minimal equipment requirements [40]. Although the most widely accessible and widespread, this approach demands considerable manual skill to produce consistent, thin sections, section quality can vary between operators and tissue types, and this can be time consuming

To address the need for more reproducible and accessible sectioning, the *Rapidtome* was developed as a low-cost, open-source alternative to conventional microtomes [40]. This device enables rapid and repeatable hand-sectioning of plant tissues, including roots, with minimal training and no requirement for fragile or high-cost components. More precise sectioning can be achieved using vibratomes and rotary microtomes. Vibratomes employ a vibrating blade to cut sections from fresh or fixed tissue [41]. In contrast, rotary microtomes are typically used with samples embedded in paraffin or resin and produce ultra-thin sections ideal for detailed histological staining and high-resolution microscopy. While these instruments yield highly consistent results, they require specialized training and are generally more time- and resource-intensive, though can be utilised in high throughput workflows [41].

The recently developed Laser Ablation Tomography (LAT) system operates differently as it combines the 'cutting' and 'imaging' steps in one interface [42]. LAT uses a powerful laser beam to create one cut surface (that can then be serially ablated in blockface fashion) through a sample, this laser near-simultaneously provides illumination or autofluorescence excitation of the ablated sample surface, while images are captured with a camera positioned to focus on the sample in the cutting plane. Typically, LAT relies on an ultraviolet (UV) laser beam, as many components of the plant root cell wall autofluoresce under UV light. However, infrared (IR) lasers have also been utilized [43]. This unique approach of using the laser for blockface ablation, as well as illumination and excitation, negates the need for sectioning and histological staining. These properties make use of LAT extremely fast to acquire high resolution cross section images. The use of ablation rather than sectioning also means large, tough, or brittle samples that may be intractable in systems requiring sectioning, can be cut and imaged with relative ease. Additionally, the use of high precision sample positioning stages enables LAT systems to be used for both two- and three-dimensional data acquisition in both longitudinal and latitudinal orientations. By substantially increasing imaging throughput, this technology makes it feasible to conduct large-scale genetic mapping studies, such as genome-wide association studies, which are critical for dissecting the genetic architecture of anatomical form and function.

Currently LAT is at the forefront of available anatomical phenotyping methods in terms of throughput, suitability in range of sample types, and resolution achievable in both two and three dimensions. Ultimately however, these systems are extremely scarce, expensive to set up, and time consuming to configure safely. Although these characteristics may limit the wider adoption of LAT for root phenotyping, there are several transferable concepts that can be integrated into more traditional anatomical phenotyping pipelines that can provide high throughput for 2D transverse section imaging. Recent advances in 3D printing have enabled the rapid prototyping of custom components for plant phenotyping, including tools that streamline sample slicing and preparation. The plant research community has embraced this technology, leading to the development of numerous guides, devices, and open-source pipelines aimed at increasing throughput and consistency in anatomical imaging. Through careful optimization of each step, it is now possible to significantly accelerate the workflow and enable high-throughput imaging of plant anatomical features.

Motivation for development of a new platform

Combining concepts from the LAT system with 3D printing and off-the-shelf, low-cost digital microscopes, we have developed a platform to obtain root anatomical images with high throughput and with sufficient resolution for trait capture. To demonstrate the utility of our platform, we present root anatomical data from a survey of historic German winter wheat cultivars, investigating inter- and intra-varietal differences in anatomy. Recent studies have shown that modern breeding practices, shaped by high-input and high-density agricultural systems, may have inadvertently selected for genotypes with smaller root systems and more conservative water use strategies [44]. It is important to increase the accessibility of root anatomical phenotyping methods; an increasing body of work has highlighted the utility of adaptive root anatomical plasticity (a change in development in response to environmental stimuli) in overcoming edaphic stresses resulting from environmental instability, and so has been proposed as a breeding target for crop improvement [33,45,46]. The plasticity described in these studies largely considers the variation in developmentally comparable roots on different plants that have experienced different environments. A further plastic characteristic is the extent of change (and rate of change per unit length) within a single root during its development [47]. Significant anatomical changes along the wheat root axis have been observed, and the amount of change shown to be affected by environmental conditions [47]. We consider these anatomical changes along the root axis to be a critical and largely unexplored dimension in understanding the functional role of root anatomy in the environment. Investigating plastic responses and evaluating their functional effects requires the ability to rapidly image large numbers of roots, quickly, consistently, and with sufficient image quality to reliably quantify anatomical traits. This need only grows when considering the opportunities presented in phenotyping root anatomy in greater resolution along the root axis.

We present an anatomical imaging platform that uses commercially available equipment in combination with custom designed 3D printed components that facilitates high throughput anatomical imaging of root tissue. We consider this Rapid Anatomics Tool (RAT) an accessible alternative to more costly anatomical imaging equipment configurations. It provides a pared back toolset well optimised for cross sectional imaging, capable of capturing root anatomical images at high throughput and of sufficient quality for detailed quantitative analysis. This platform was validated by investigating anatomical variation in diverse germplasm to assess its suitability, and by performing cross-platform validation against hand sections and transmitted light microscopy. We believe our RAT platform to be innovative and functionally distinct from existing platforms due to: 1) the integration of the sectioning apparatus with the imaging stage, 2) stain free imaging, and 3) the low cost of and high throughput of the platform.

MATERIALS AND METHODS

Overview

The Rapid Anatomics Tool (RAT) is a platform designed for fast, high-quality anatomical imaging. Its efficiency comes from combining two key principles: blockface-like imaging and stain-free imaging using near-ultraviolet (nUV) autofluorescence.

Blockface-like Imaging

Our method is inspired by blockface imaging, a technique where a sample, typically held in a supporting matrix, is cut to remove a layer and expose a new, internal surface [48]. The image is then captured directly from this freshly exposed face of the remaining sample block. Typically, blockface imaging is used in conjunction with serial sectioning to obtain 3D structural information.

This approach is also used in techniques like Laser Ablation Tomography (LAT) to generate 3D structural information. This differs from many cross-sections anatomical imaging methods where the part of the sample imaged is the thin section cut away from the bulk of the sample, which is often done so that the section can be stained or for transmitted light microscopy. With the RAT system, the sample is positioned in a holder, precisely cut to reveal a crisp and clear cellular face, and this exposed surface is imaged.

nUV autofluorescence imaging

Several high throughput root anatomical imaging platforms (including LAT) make use of natural autofluorescence of root cell walls under ultraviolet (UV) or near-ultraviolet illumination (nUV) [49–53]. In many sample types, this can replace the need for staining with chromatophore or fluorophore dyes, reducing the steps required between sample collection and imaging.

By integrating a rapid blockface imaging workflow with stain-free nUV autofluorescence, the RAT platform achieves a unique combination of high speed, high quality, and high throughput for anatomical studies. While the core principles of direct blockface imaging and nUV autofluorescence are versatile, in this paper, we present a specific suggested setup. These concepts can be adapted for a variety of equipment and imaging systems to study root anatomy and could potentially be extended to the rapid anatomical analysis of other plant organs.

Experimental and Technical Design

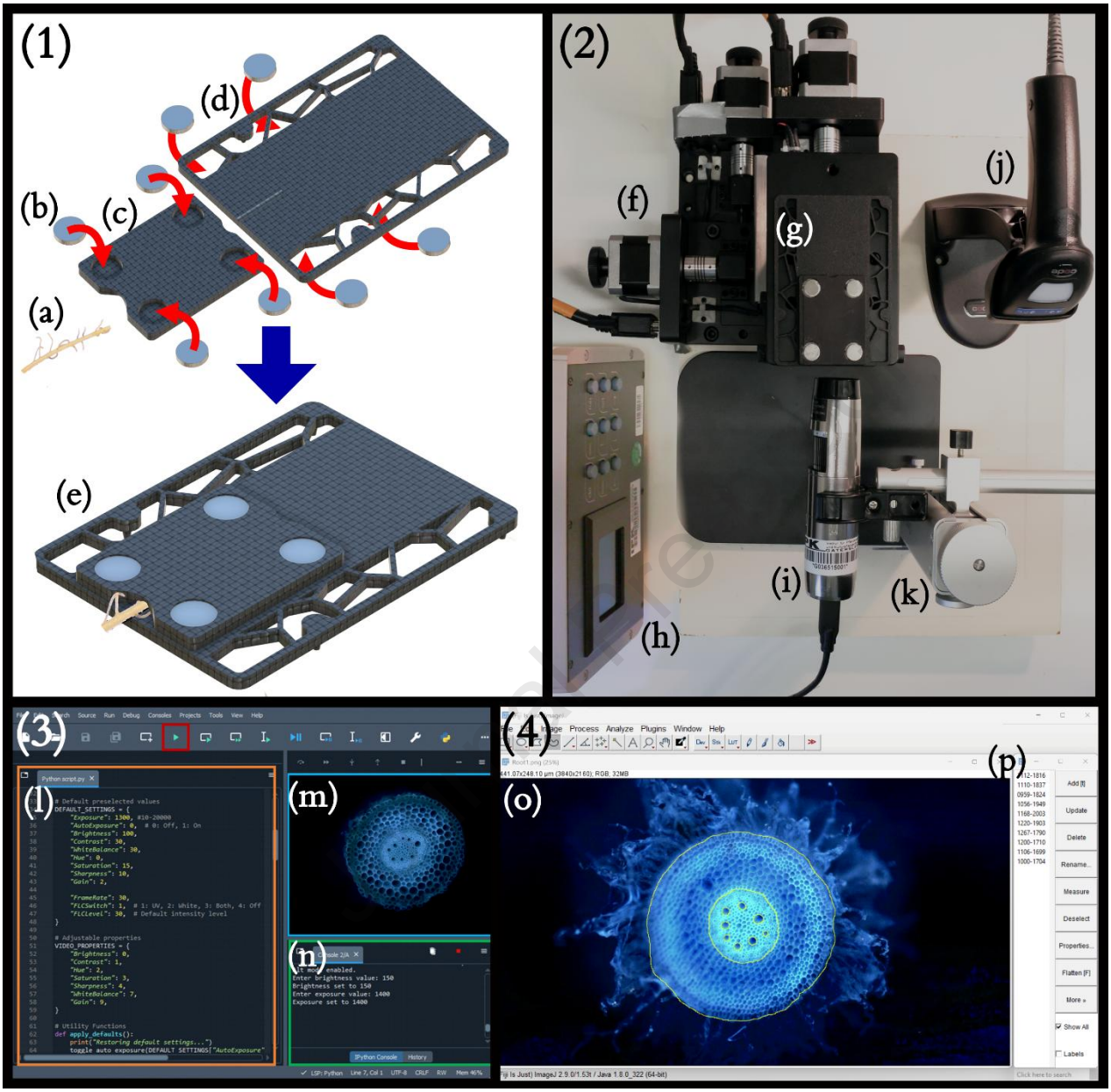

Figure 1: Rapid Anatomics Tool (RAT); Sample holder and hardware assembly, image capture and measurement system; (1): 3D printed sample holder components (black) magnets (grey) and root segment), (a) 3 cm root segment, (b) 2 mm x 10 mm disc magnet held in place with superglue in the inset voids (red arrows), (c) 3D printed lid plate, (d) 3D printed base plate, (e) complete RAT root holder assembly, (2): Top-down image showing full hardware setup used in this manuscript, including (f) motorized positioning stage, (g) complete RAT root holder assembly, (h) motorized stage controller, (i) USB microscope, (j) 2D barcode reader, (k) USB microscope holder, (3): Python based USB microscope control script run in Spyder-IDE 6.1, consisting of (l) an editable script showing default camera settings, (m) live video window from camera showing sectioned root, (n) console reporting current applied settings and successful image capture, (4): Image analysis using Fiji (ImageJ), (o) tissues annotated and measured in study, (p) ROI manager used to store image annotation polygons

We present a guide for assembly of the equipment for (**Figure 1**) and utilization of an anatomical imaging platform. This uses custom designed tools and accessible commercially available equipment to enable a hand slicing based workflow to achieve rapid and quality root anatomy image acquisition. Full details of hardware specifics, supplier, and prices are given in the S2 materials ('S1:Equipment List').

Imaging hardware

In our protocol, we use an 8-megapixel USB microscope, with variable magnification 1 X to 220X, with an inbuilt nUV (375 nm) ring light surrounding the objective (Dino-lite Edge AM8517MT-FUW), connected to a standard windows desktop PC. To hold the microscope in place, we use the holder from the microscope manufacturer, though a lab retort stand would function similarly. The manufacturer also provides a software development kit (SDK) that can be used to create custom software control solutions.

Sample positioning stage

Fine control of sample position is an important element in imaging microscopic structures, in centring the subject of the image, as well as bringing the subject into the correct focal plane. Motorized and computer-controlled stages enable reproducible and precise small movements, and create the opportunity to automate aspects of the sample location process. We have optimized our platform around the use of an XYZ motorised control stage, comprising two stacked linear actuator stages with a 50 mm travel range, with a motorized lab on top, these three axes are connected and controlled by a motion controller. The stage manufacturer also provides a software development kit, enabling custom workflows and control of the stages over serial port as well as through their software. Alternatively, we have found the manual positioning stage available from the microscope manufacturer works well and provides sufficiently easy fine manipulation of sample position for use across the full range of magnification levels, and Z axis adjustment can be provided by the microscope stand. Further, many multi-axis fine positioning stages are available commercially or can be manufactured using 3D printing. In order to be amenable with our suggested workflow, a stage should have mounting holes on the top surface, be made of a non-magnetic material, for the mounting holes to align perpendicular to the base, that the base aligns well with the microscope holder, and that the surface of the multi-axis positioning stage have an area greater than 4 cm by 6 cm.

Sample holder concept and production

The throughput of the LAT system is in part achieved due to the consistency in position of interchangeable samples and the cut surface thereof to be imaged relative to the imaging equipment. To achieve this in our platform, we designed a sample holder and manual sectioning jig, intended to achieve the following objectives: 1) to hold a sample of root tissue of a range of sizes sufficiently securely for it to be cut in place without sample movement within the holder, without causing mechanical damage of the region to be imaged; 2) to facilitate cutting of the sample to a consistent fixed protrusion from the sample holder; 3) to locate consistently in a set position relative to the imaging equipment without affecting quality of the image of the sample.

The sample holder was designed for 3D printing in two parts, a base plate with conical 'feet' that locates to the mounting holes on the sample stage, and an attachable lid, between which the root sample to be cut and imaged is sandwiched (Figure 1). The sample holder base was designed with a grooved indent in the top surface to help align the sample with the midpoint of the plate consistently. A variety of lids were designed with corresponding recesses with a range of depths to

accommodate different diameter roots. The base plate was designed to sit on top and cover the sample positioning stage, and for the sample (before cutting) to overhang the front edge of the base where it would face the camera, we found a size of 7 cm by 12 cm convenient to this end and easy to handle. Lids were designed so the front edge of the lid sat 1 mm recessed from the front edge of the base when the magnets were aligned. Lids were designed to clamp a rear portion of root tightly in place, and for a forward portion of the root to be unclamped and undistorted. As 2 mL microcentrifuge tubes are (in the experience of the authors) the most common vessel for storage of samples for root anatomical imaging, and these typically have an internal depth of approx. 3 cm, lids were designed to hold roots of that length, with 5-10 mm protruding from the front of the base and lid plate sandwich.

On opposite sides of the lid and the base, 2.4 mm deep by 10.4 mm wide cylindrical voids were left, to accommodate 10 mm by 2 mm disc magnets. (A note on assembly: magnets were fixed in place using cyanoacrylate superglue, and we advise preparing the base first, one magnet at a time, then each lid separately, using the base to hold the magnets in the lid plate in place.)

The printer used to produce the sample holders was a Bambu Lab X1C. All settings used were default recommendations of the printer management software per plastic type used. Best results were achieved by printing the base plate (Supplementary Material: 'RAT_Base_plate(DinoLite_manual_stage).stl', 'RAT_Base_plate(motorized_stage).stl')in black PLA-CF filament, a polylactic acid-based filament with 5-10% by weight carbon fibre composition. This is abrasion resistant, prints with minimal layer lines, non-fluorescent under UV lighting, matte and non-reflective, suitable for sanding, adheres well with superglue, and prints with a low degree of shrinkage meaning modelled components came out true to size. The lids (Supplementary Material: 'RAT_Lid_X.stl'), also printed well in PLA-CF for the same reasons, though for large samples (>6 mm diameter) additional styles of lids were designed to avoid compressing any part of the sample. This was not usually an issue with the small to moderate (0.1-6 mm) diameter roots, but with larger samples, compression of one region occasionally resulted in guttation causing fluid build-up on the cut surface. In these cases, using holders printed using TPU (thermoplastic polyurethane), a soft and more flexible plastic, worked well, though glue adhered less well to this material. The optional blade holder (Supplementary material S2: Assembly and Use Guide), can be printed using any rigid plastic.

This is the equipment configuration as used and recommended by the authors, however exact shape and material of the sample holders, assembly of sample positioning stage, and even model of microscope can be amended as to requirements or availability.

Biological sample preparation

We have used this method or minor variations thereof to successfully section and image thousands of root cross sections for analysis; with sample sizes ranging from 100 µm to 20 mm in diameter. These samples have come from plants grown under varied growth conditions ranging from roots excised from freshly germinated seeds to in-vitro tissue culture, hydroponic culture, compost and sand in controlled environments, as well as from field conditions. Thus far we have found that mature root tissue, outside the root tip and elongation zone, yields the best results, and that image quality diminishes close to the apex. Furthermore, while samples could be processed as fresh tissue, we have noted a tendency towards an increase in image quality after samples were stored in preservative solution for a period of time. For this typically we have subsampled a length of root 2-3 cm long, and stored this in a 2 mL microcentrifuge tube. Tubes are labelled with the corresponding sample name printed on an ethanol resistant sticker label, featuring a 2D Quick Response (QR) code graphic encoding the sample name on the label.

To preserve the sample, we have used solutions of ethanol, ranging from 45% to 70% v/v (depending on availability, transportation needs, and duration of storage intended) filling the remainder of the volume of the tube, and found that a period of one to two weeks at 4 °C yields samples with higher lumen to cell wall contrast than fresh tissues. Roots could be stored for longer periods of time than this (we have not been able to observe age related deterioration in anatomy even in samples stored over 6 months), but 2 weeks was typically sufficient depending on sample size.

Starting with a clean (i.e. free of soil and growth medium) 3 cm length of root, having been stored in ethanol solution for prerequisite time, sample preparation is then straightforward. The root sample is removed from the ethanol solution, handled by the extremities of the sample, and gently blotted on tissue paper (dust free technical wipe paper so as to not transfer UV fluorescent particulate to the sample). The sample is then positioned on the sample holder base plate on top of the indented groove at the front end of the plate with 5 to 10 mm overhanging from the front, making sure to orient the overhanging region perpendicular to the front of the sample holder (**Figure 1**). An appropriate lid plate can then be selected with a sufficient recess to hold the root firmly without crushing the region at the front of the holder. While holding the base plate *in situ*, the lid plate can then be placed on top of the root.

Sample Cutting

With the root clamped firmly in place, the root can be cut to length and a fresh surface exposed for imaging. The objective is to obtain a clean cut with minimal damage to the sample and for high throughput processing, for the cut surface to be in a consistent position relative to the sample holder, so minimal sample repositioning and focus adjustment is required.

To achieve this, roots are cut in line with the front of the sample holder base plate. For small to medium sized roots (0.1 to 4 mm), roots can be easily cut by running a Teflon coated single edge safety razor over the front of the holder assembly. Holding the edge of the razor flush with the base plate, and at a 45-degree angle bringing this across the sample with a slight downward motion we found normally gives a clean cut, though this can be adjusted to individual preference. For thicker roots, a thinner blade i.e. half a double-sided razor blade can achieve better cuts. As these can be hard to hold and use loose, we designed a 3D printable razor holder (Supplementary Material: 'RAT_razor_holder.stl'). The frequency with which the blade will need to be replaced depends on the toughness and size of the samples being processed, for thick field grown roots this may be as frequent as every ~5-10 samples, and thinner and or artificial media grown roots every ~20-40 samples. Once the sample is in the holder and cut to length, the holder unit can be mounted in front of the microscope on the sample positioning stage.

Staining

By using nUV illumination, the need for further contrast staining is eliminated for a large range of root sample types, particularly mature Poaceae axial root samples. This method however is less suitable for visualising tissues that have less secondary thickening of their cell walls, and typically those of a younger developmental age.

To expand the potential range of uses of this setup, we tested several other sample types and found that the autofluorescence in the cortices and the contrast between the cell walls and the lumen in these tissues were poor. To overcome this, we found a short, direct application of 0.5 µL aqueous solution of fluorescent brightener 28, 0.3 mg mL^{-1} to the cut face, letting this sit for approximately 10 s (adjusted to specific samples where needed), followed by gentle rinsing of the sample in the

holder with water and light blotting of the sample holder with tissue paper to remove excess water, enough to improve the fluorescence of the sample to enable imaging. This required readjustment of the image capture settings to account for the change in type of fluorescence, and results in a partial loss of the differential fluorescence between secondary thickened and non-secondary thickened cells but did enable previously poorly visible cells to become clear.

Image capture

The digital microscope camera is provided with software (Dino-Capture) of which two versions exist (as of date of submission) (2.0 v 1.553B, and 3.0 v1.1.1.3) (Supplementary Material: 'S3: Software List'). We have found version 2.0 more robust and customisable in our use cases, with the ability to add keyboard shortcuts useful to achieving high throughput imaging (Supplementary Material: 'S4: Imaging and Software Control'). That said, we felt that with our specific use case of trying to capture images in high throughput for analysis, improvements could be made. There is a software development kit (SDK) available for the microscope, available for use with LabView (National Instruments) application development software, as well as suitable for use with Python programming language, among others.

To reduce software control steps in our imaging platform, we produced an application to be run in Python, displaying a live camera feed, giving the ability to adjust camera parameters and image capture triggered by text entry (Supplementary Material: 'RAT_DinoLite_Custom_Workflow_Controller.py'). This application is a basic deployment of the software development kit, with minimal front-end development for simplicity, and no graphical user interface. When executed, the script opens a live preview of the video feed from the camera, which once open, camera settings can be changed and image capture can be triggered. There are two 'modes', capture mode, where image capture is triggered by text entry, and 'alt-mode' where hardware settings can be altered in the python console which is toggled between by the 'alt' key. In alt-mode, the viewing window must be selected, then keyboard shortcuts (Supplementary Material: 'S5: Custom Software Control'). can be used to change illumination settings as well as camera settings such as exposure, brightness, gain, and frame rate, or apply defaults as set in the python script.

Our recommended workflow includes use of a 2D barcode reader to scan the label on the sample tube; with this system image capture is triggered by text entry followed by a 0.1 second pause, saving the image with the scanned code text or entered text as a TIFF file, with the metadata of the image field of view, pixel size, and current magnification level, saved as metadata in the image. The digital microscope camera settings can be adjusted ad hoc during imaging as required by the sample type.
Compared to the provided software, this workflow with the python script and 2D barcodes enhances throughput in several ways. Firstly, when using a manual stage, the scanning of the barcode triggers automatic image capture and therefore file saving and naming is not only faster and less susceptible to error than doing this manually, but also makes the process keyboard and mouse free. This reduces the steps and time required per image captured, and reduces a potential source of camera vibration. Secondly, the script saves these images directly as .TIFF files with metadata about the hardware setup embedded, this improves the reproducibility of image capture and allows the settings used for imaging to be readily checked in any viewer rather than only with the provided software. Thirdly, the scale is included in the metadata with the images captured in this format with, therefore these images do not need additional export or conversion before they can be measured, speeding up this part of the process too.

Plant samples

We performed two independent demonstrations of the suitability of The RAT platform for anatomical analysis, and furthermore we have tested a range of diverse plant samples, across multiple devices and set-ups. We performed a cross-platform comparison between the RAT and thin sections imaged using transmitted light using *Tripsacum dactyloides*, and inter-cultivar and analysis of two German winter wheat varieties, S. Dickkopf (released in 1895), and Tommi (released in 2002), investigating inter- and intra-varietal differences in anatomy.

Cross-platform validation using *Tripsacum dactyloides*

Plant cultivation and sampling

Clonal ramets of *Tripsacum dactyloides* accessions from a diversity panel in Lawrence, Kansas, were transplanted in August 2023. Plants were placed into pots (10 × 10 × 24 cm) filled with local topsoil and allowed to acclimate for two months at a field plot at the University of Kansas Medicinal Plant Research Garden (39.0101, −95.2072). Subsequently, plants were transferred to a climate-controlled greenhouse (16 h/8 h light/dark, 28 °C/22 °C) for three weeks prior to a 72-hour waterlogging treatment. At harvest, shoots were removed and roots were washed free of soil, then stored in 75% (v/v) ethanol. From each plant, a nodal root exceeding 8 cm in length was selected; if multiple roots met this criterion, the root with the greatest diameter was chosen. When no nodal root exceeded 8 cm, the longest available root was used. For anatomical measurements, 1 cm segment was excised from the root base (i.e., 1 cm from the point of attachment).

Imaging and analysis

Twenty-two root segments were hand-sectioned transversely using a Teflon-coated razor blade and mounted in distilled water for imaging. Sections were imaged at 20–40× magnification using an upright microscope (3000-LED) equipped with a camera module (ExcelisHD/4K; ACCU-SCOPE Inc., Commack, NY, USA). The remaining portion of each root was imaged using the RAT platform using the described sample mounting, cutting, and imaging methods (Supplementary Material: 'Cross-Platform_Comparison: Figure 1). Section images were analysed using ImageJ. Measurements included the total root area, stele area, metaxylem vessel area and number, and aerenchyma lacunae area, using polygon area selections for each trait. All images were calibrated to convert pixel measurements to micrometres.

Wheat root anatomical analysis

Plant growth and sampling

Plant growth, management and above ground traits are described in Behrend et al. 2025 [54], and key details are as follows. Plant material was obtained from a field experiment at the research station of the University of Bonn, Germany, Campus Klein-Altendorf (50°37' N, 6°59' E). The experimental station is located inside the temperate oceanic climate zone with average long-term annual precipitation sums of 603 mm and a mean yearly temperature of 9.4 °C between the years 1956-2014. Mean annual temperatures during the experimental years were 11.5 °C and 12 °C, with total annual precipitation sums of 723 and 824 mm during the two experimental years of 2023 and 2024 respectively. The soil at the experimental station is classified as a Haplic Luvisol derived from loess and considered to be homogenous and fertile. A detailed description of the physical and chemical soil properties at the experimental station is provided in Vetterlein et al. 2013 [55]. The experiment in which the winter wheat cultivars were grown was arranged in a

complete randomized block design, with four field repetitions. Management of the field experiment was handled in a conventional manner to minimize nutrient, pest and disease stress and competition. A detailed description of the management of the field experiment, including sowing dates, pre-crops and dates and application rates of other management interventions such as the application of mineral fertilizers and fungicides, herbicides and growth regulators can be found in Behrend et al. 2025 [54]. Cultivars used in the experiment were selected as they were among the most widely cultivated varieties during their release periods [56]. Additionally, they were previously grown as part of a long-term fertilization study [57] and as such were previously included in other studies that investigated breeding effects and their interactions with management interventions on winter wheat yields [58,59].

Samples were collected as described in Baca Cabrera et al. 2025 [44] using a slightly modified version of the wheat root excavation method described by York, 2018 [60]. Sampling took place at the end of the tillering stage (BBCH < 30) during two growing seasons, specifically in spring 2023 and spring 2024. All winter wheat cultivars were sampled simultaneously during single-day campaigns. A representative area within each plot was excavated, targeting the top 20–30 cm of soil and covering a similar diameter (around 30 cm). Due to the high planting density, each collected sample typically included 5–10 plants. The excavated plants were placed into sample bags, transported to the laboratory, and kept at 5°C until they could be processed. In the lab, the samples were first soaked in water and then carefully washed. Root crowns were then separated from the shoots near the base, leaving approximately 3 cm of tiller shoot tissue attached, and stored again at 5°C in a solution of water (37.5%), ethanol (37.5%), and glycol (25%). For further analysis, four plants per plot were preserved.

Subsampling for anatomical imaging

Four of these preserved roots per plot were stored in a 30 mL vial in the ethanol, water, glycol solution until subsampling. Each root was dissected into three 2.5 cm lengths, a basal (the 2.5 uppermost cm of the root), middle (from the middle of the root sample, typically 10-12 cm from the base), and a tipwards sample (2 cm towards the middle from the distal most region present, typically 20 cm from the base and or 3 cm back from the root tip). It should be noted that the samples usually did not include the tip, due to the roots having been excavated from the field. These samples were transferred to a 2 mL Eppendorf microcentrifuge tube, and the remainder of the volume was filled with 70% ethanol (v/v) solution. Each root from each pooled plot sample was assigned its own identifier number, and each root position was categorized separately. Sample tubes were labelled with a QR code giving the sample name. Samples were stored at 4 °C in the ethanol solution for a minimum of two weeks.

Anatomical imaging

Roots were prepared and imaged as described above N=32 per genotype and sampling position. Root samples were largely consistent in diameter, so the digital microscope was used at maximum magnification (220x) for the whole sample set. A small number of samples (< 2 %) had poor cortical autofluorescence, so the staining procedure was used in these cases. This did not affect measurement.

Root anatomy image measurement

Images were measured manually using FIJI (ImageJ distribution) [61]. After image capture, all images (n=573) were saved as a multi-slice '.TIFF ' file, with image names as slice labels, which were recorded then hidden. This image stack was then converted to 8-bit to reduce file size and

facilitate threshold based automatic selection. Image features were annotated one feature at a time across the whole stack using the region of interest (ROI) manager to record annotations. All traits were selected using polygons for area measurement, recording the image feature in pixel coordinates and with measurements exported in square millimetres. For an example of feature annotations please see 'Supplementary Material: S6 Image Annotation and Measurement'. Total root area was annotated using manual selection tools (freehand selection, ellipse), to outline the root with a selection, which was then added to the region of interest manager, and then the stack was progressed one slice. This annotation took 5-10 seconds per image. Once root area was measured in each image for the whole stack, the contents of the ROI manager was saved to a .ZIP file, preserving the polygon co-ordinates, and the measurements of each slice were exported by selecting all ROIs and running measure. The ROI manager was cleared, and this process was repeated for stele area from the first image to the last, creating a second ROI .ZIP file. Metaxylem were annotated individually, adding each metaxylem to the ROI manager. To facilitate this, the image stack had a 2-pixel radius gaussian blur applied, enabling smoother threshold selections. Using the 'magic wand' tool, a point in the lumen of each metaxylem was selected with a threshold of 20, this typically created a selection that included the whole metaxylem lumen, and where needed this was adjusted *ad hoc* to select the whole cell contents, otherwise a different point nearer closer to the cell wall was selected. If threshold-based selection failed (<1% of the time), manual selection as with the root and stele were used. Every metaxylem was annotated in each image in this way. The time this took per image varied with the number of metaxylem in the image, however this was typically 3-5 seconds per metaxylem. The complete list of metaxylem ROIs were measured and saved as a third .ZIP file. A graphics tablet with programmable hotkeys (Huion 1060P) was used to accelerate these annotations; polygons were added to the ROI manager with (t), and the image sequence was progressed with the (>) key. Annotation of each image typically took 30-60 seconds per image in the stack. In addition to speed, this system has the further advantages of effectively blinding the measurements, reducing the complexity of each measurement step and the opportunity for bias in the way each trait is annotated relative to others. This also allows for easy re-export of measurements, and a high degree of potential for downstream interoperability, or further independent annotations.

Data processing and analysis

Image data was processed in Microsoft Excel (2019) to create summary data for each image, for each cultivar, and each root position. Yamauchi *et al.* [10] used the ratio between different tissue types within the root to explore diversity in adaptation of Poaceae across an environmental water availability gradient. We have used two of these metrics (xylem to stele ratio, and cortex to stele ratio), multiplied to give a single value (XCS, $(Xylem\ area \times Cortex\ area) \div Stele\ area^2$) which we found served to aid in identification of trends in change of the proportional relationship between tissues comprising the root cross-sectional area. Data was analysed and statistical comparison of anatomical traits between cultivar and position was carried out with two-way analysis of variance (ANOVA) with Tukey's multiple comparison correction in Prism 10 (GraphPad) P=0.05.

RESULTS

Efficacy of RAT platform

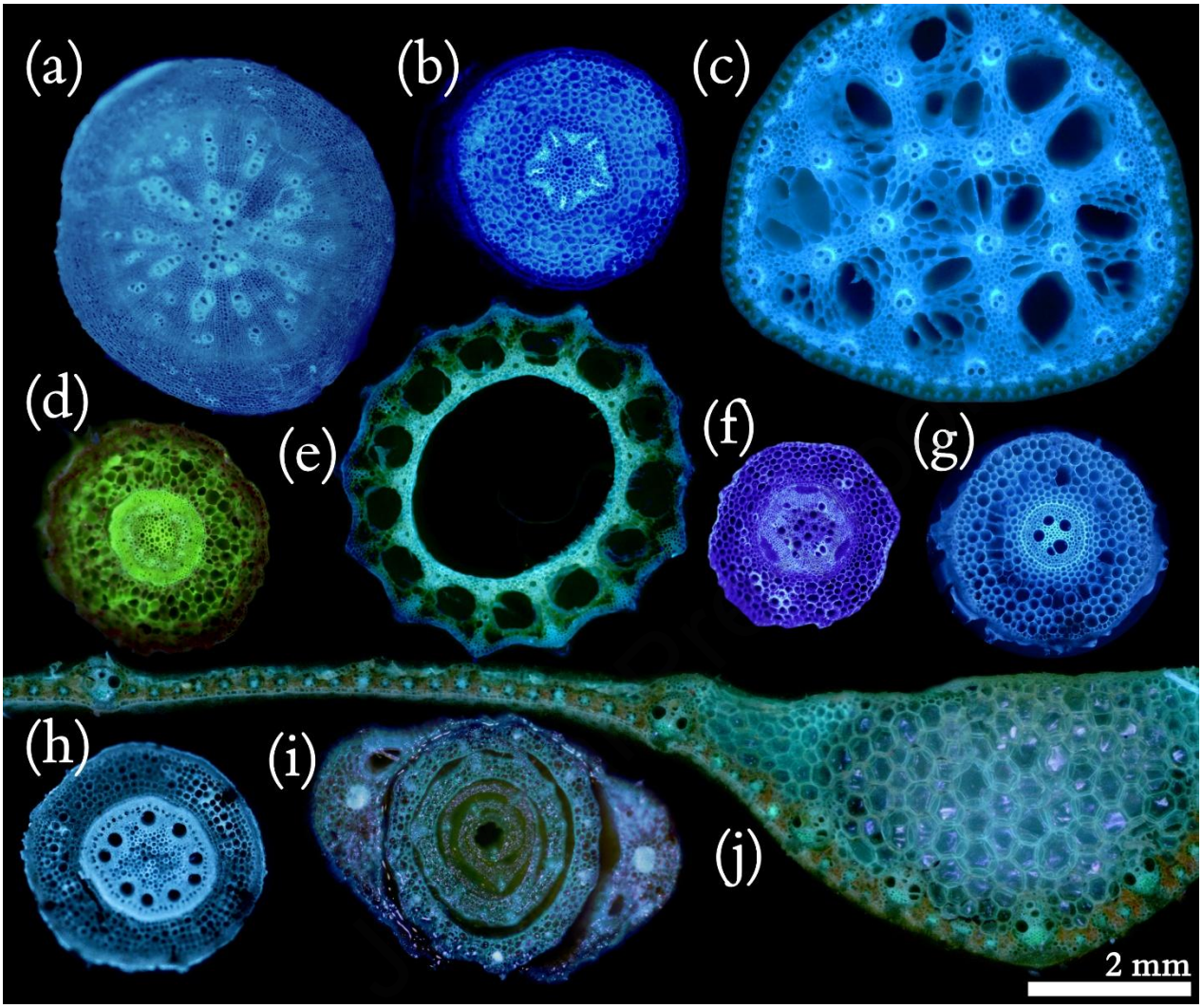

Figure 2: Anatomical images of transverse sections through various plant organs captured using RAT platform; (a) horseradish (*Armoracia rusticana*) primary root, (b) Cassava (*Manihot esculenta*) adventitious root, (c) papyrus (*Cyperus papyrus*) stem, (d) Saxifrage (*Saxigraga stolonifera*) stolon, (e) Horsetail (Equisetum) stem, (f) Pea (*Lanthrus oleraceus*) adventitious root, (g) Wheat (*Triticum aestivum*) adventitious root, (h, i, j) Sorghum (*Sorghum bicolor*), (h) adventitious root , (i) seedling stem, and (j) flag leaf; Scale bar 2 mm.

The described image acquisition platform using the rapid anatomics tool is suitable for imaging a wide range of plant samples at sufficient resolution to enable quantification of cellular anatomical traits. We have used this platform to image thousands of root sections for analysis, from species including wheat (*Triticum aestivum*), sorghum (*Sorghum bicolour*), maize (*Zea maize*), cassava (*Manihot esculenta*), and gamagrass (*Tripsacum dactyloides*), and have validated its application with stems, leaves, petioles, and storage roots, from different organ ages. Representative images showing some of the range of species and sample types are shown in **Figure 2**. This platform as described is well optimised for capturing single cross sectional 2D images from a sample in high throughput, and with a low hardware and running cost as well as a shallow learning curve. With just a small amount of practice, researchers without prior experience of anatomical imaging or

microscope use can acquire high quality cross section images, and with greater practice, achieve high throughput (~45 samples per hour for a single user) in doing so.

Cross-platform comparison

Analysis of the root anatomical features measured using images captured with the RAT platform and the transmitted light microscope showed extremely high significant correlation for all traits, and very high agreement in absolute values (Supplementary Material: 'Cross-Platform_Comparison: Figure 2'). All trait correlations had a Pearson correlation r value of greater than 0.95, and a P-value of <0.0001. There was no significant effect of the platform used on measurement of root area, stele area, or metaxylem number, however in the transmitted light images measured metaxylem area was on average 13% larger than in the RAT images, and aerenchyma area was 18% larger in the transmitted light images (Supplementary Material: 'Cross-Platform_Comparison: Table 1'). Despite the significant difference in areas, the correlation between these features cross-platform was still very strong with r values 0.97 and 0.96 respectively.

Differences in root anatomy between cultivars

As a proof of concept, root anatomy was evaluated in crown roots of two German winter wheat cultivars (*T. aestivum L*) one historic (S. Dickkopf, released in 1895), and one contemporary (Tommi, released in 2002), in multiple positions along the root axis. This analysis revealed significant differences between cultivars, as well as significant differences in anatomy along the root axis, and difference in the propensity for change along the root axis between the cultivars.

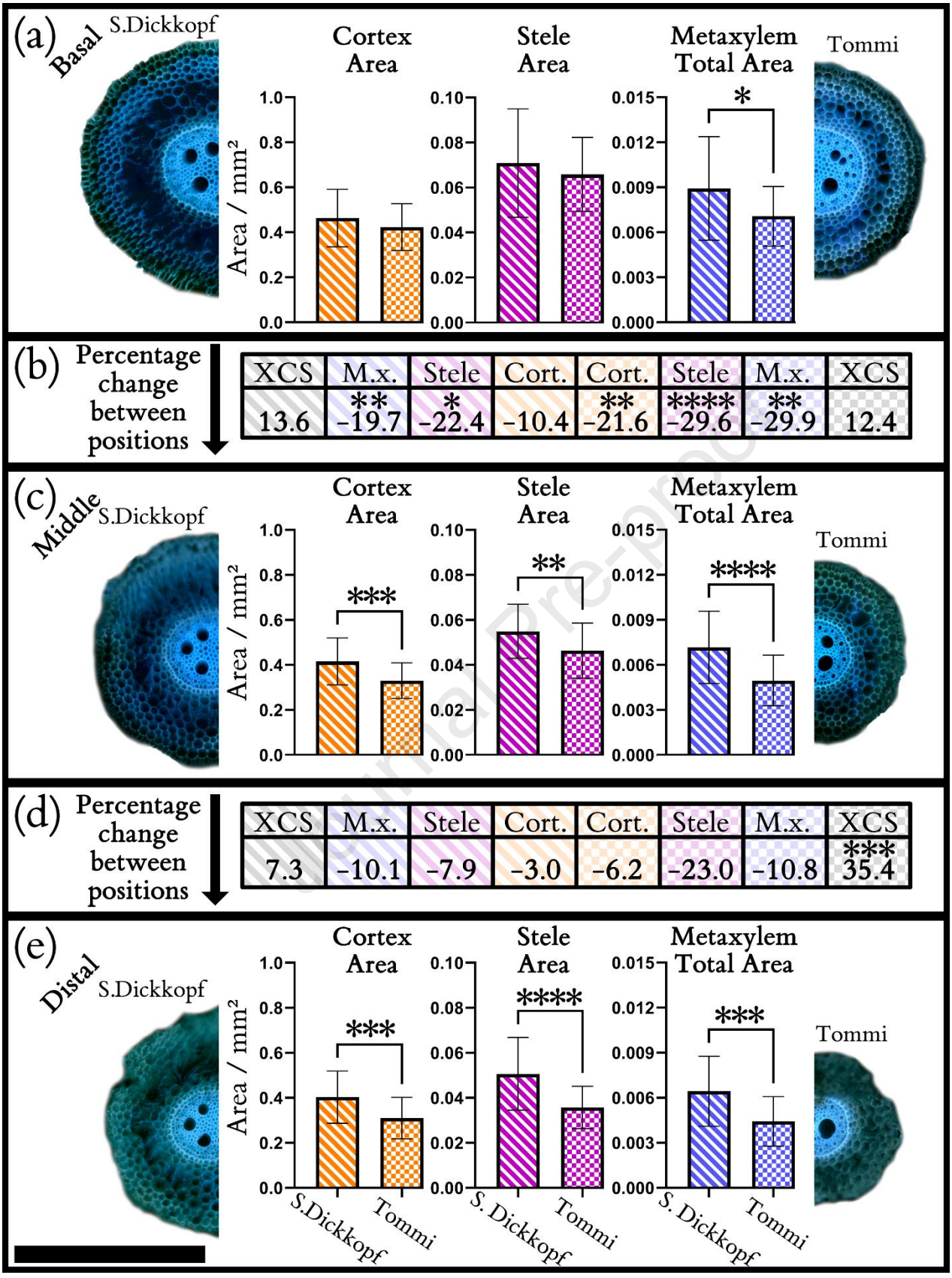
(a)
Basal
S.Dickkopf
Cortex Area
Stele Area
Metaxylem Total Area
Tommi
Area / mm²
1.0
0.8
0.6
0.4
0.2
0.0
0.10
0.08
0.06
0.04
0.02
0.00
0.015
0.012
0.009
0.006
0.003
0.000
*
(b)
Percentage change between positions
XCS | M.x. | Stele | Cort. | Cort. | Stele | M.x. | XCS
13.6 | ** −19.7 | * −22.4 | −10.4 | ** −21.6 | **** −29.6 | ** −29.9 | 12.4
(c)
Middle
S.Dickkopf
Cortex Area
Stele Area
Metaxylem Total Area
Tommi
***
**
****
(d)
Percentage change between positions
XCS | M.x. | Stele | Cort. | Cort. | Stele | M.x. | XCS
7.3 | −10.1 | −7.9 | −3.0 | −6.2 | −23.0 | −10.8 | *** 35.4
(e)
Distal
S.Dickkopf
Cortex Area
Stele Area
Metaxylem Total Area
Tommi
***
****
***
S.Dickkopf
Tommi
S. Dickkopf
Tommi
S. Dickkopf
Tommi

Figure 3: Root anatomy differs between two German winter wheat cultivars and along the root axis within cultivars; Panel (a), (c), and (e) show anatomical differences between cultivar within the same sampling position. Panels (b) and (d) show the percentage change in mean trait value between positions in each cultivar. Traits and abbreviations include Cort= Cortex area, Stele= Stele area, M.x.= Metaxylem total area, and XCS= Ratio descriptor of (Meta)Xylem, Cortex, and Stele areas. In all panels, the left side and descending stripes represent S. Dickkopf (1895) and the right side and checkered pattern, Tommi (2002); colours indicate the anatomical region with orange representing the cortex, magenta representing stele, and blue representing metaxylem total area. (a) Root anatomy in basal root region, (b) Percentage change in mean trait values between basal and mid-root samples within cultivars, (c) Root anatomy in mid-root region, (d) Percentage change in mean trait values between mid-root and distal samples within cultivars, (e) Root anatomy in distal root region. , Significance was determined by two-way anova with Tukey multiple comparison test comparing mean values between cultivars and positions,(* = $p<0.05$, **= $p<0.01$, ***=$p<.001$, ****=$p<0.0001$, n=32). Error bars indicate standard deviation.

Root anatomy differs between cultivars

Significant differences in root anatomical traits were present between cultivars at all three subsampling positions along the root axis. In all instances of significant and non-significant difference, tissue cross sectional area was greater in S. Dickkopf than in Tommi (**Figure 3**). In the basal region of the root, this was only significant for metaxylem total area, and in all other sampling regions, this was significant for all cortex, stele, and total metaxylem area.

Root anatomy varies along the root axis

There is a clear trend of a decrease in cross sectional area along the root axis in sampling points further from the root base. In S. Dickkopf the changes in cross sectional area between positions are only significant in the metaxylem and stele, between the basal and middle sample points. In Tommi, root anatomy changes significantly between the basal and middle positions, reflected in a significant decrease in area of stele, cortex, and metaxylem. Though there is a sizeable further percentage decrease in stele area (-23 %) between the middle and tipwards region, this change is non-significant (**Figure 3**).

Cultivars show different dynamics of anatomical transition along the root axis

To understand whether these differences in tissue areas between cultivars and along the length of the root represent a shift from isometric to allometric scaling, we used a combination of tissue ratios shown to be effective in relating anatomy to environmental adaptation (the ratios of metaxylem to stele, and cortex to stele) to derive a single value metric. This analysis shows several further distinctions between the cultivars. Firstly, Tommi, undergoes a larger change in root anatomy along the root axis than S. Dickkopf. The magnitude of change in tissue area and XCS ratio between positions along the root was greater in Tommi, than S. Dickkopf in all instances bar XCS between basal and middle sections. The incidence of significance differences in tissue areas between positions is also higher in Tommi than S. Dickkopf. The difference between the cultivars in change in tissue ratios between sample points is notable and further highlights the differences between the cultivars. Basal to middle ΔXCS is comparable and non-significant for both cultivars, however between the middle and tipward section ΔXCS is much higher in Tommi and statistically significant (**Figure 3**). This describes a significant difference in the type of scaling in the change along the root axis from isometric to allometric, between S. Dickkopf and Tommi respectively.

DISCUSSION

In this study, we present the Rapid Anatomics Tool (RAT), a novel, low-cost, and high-throughput imaging platform, and demonstrate its utility by investigating anatomical variation along the axis of adventitious roots in two winter wheat cultivars Our work provides two principal contributions: first, a significant methodological advancement that makes rapid root anatomical phenotyping more accessible; and insights into how root anatomy varies within a single root, revealing distinct patterns between cultivars, reflecting the need for more comprehensive sampling approaches when investigating the effect of anatomy on root physiology.

The platform presented here offers a rapid, low-cost, and high-throughput approach for imaging (primarily) root anatomical traits by harnessing the natural autofluorescence of lignified and suberized tissues under UV illumination. This approach largely eliminates the need for chemical staining or high-end microscopy equipment, addressing major limitations in throughput and accessibility that often constrain anatomical phenotyping in root biology.

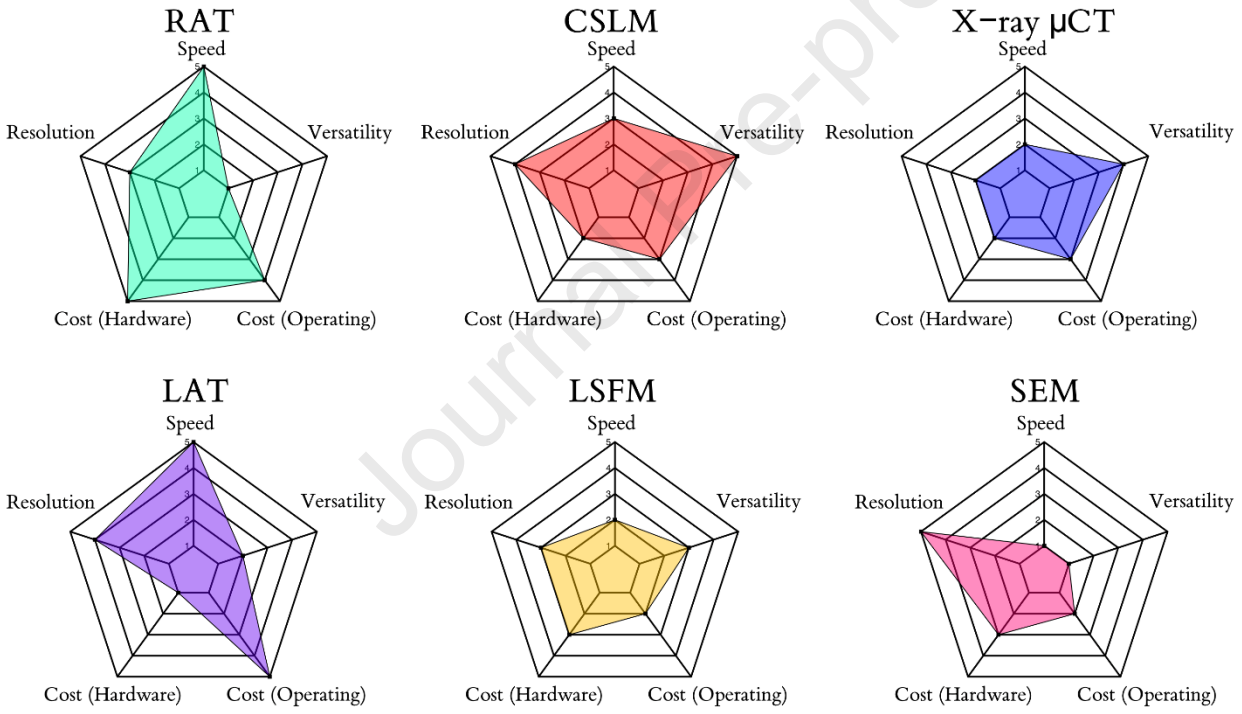

Figure 4: Illustrative plot showing the trade-offs and merits of the low-cost RAT platform relative to the advantages offered by state of the art methods for root anatomical imaging. Left to right, top to bottom; RAT: Rapid Anatomics Tool, CLSM: Confocal laser scanning microscopy, X-ray µCT: X-ray micro-computed tomography LAT: Laser Ablation Tomography, LSFM: Light Sheet Fluorescence Microscopy, SEM: Scanning Electron Microscopy. Each quality (speed, resolution, versatility, cost (hardware), and cost (operating)) was scored from 1 (innermost ring) to 5 (outermost ring) with 1 being the least desirable ((slow sample preparation, low imaging resolution, expensive hardware, expensive to operate, or limited range of applications of the techniques) and 5 the most desirable (fast sample preparation and image acquisition, low hardware cost, high micron/pixel, expensive to operate hardware, or high application beyond acquisition of 2D anatomical images). The relative merits of key attributes were assigned based on reviewed literature [1,15,21,24,29,59,60,61,62,63].

In comparing the RAT platform to microscopic imaging with transmitted light we observed a very strong degree of correlation between these systems, and broadly a high degree of agreement between absolute values. The image features that differed most were the metaxylem, and aerenchyma area, though these still correlated significantly with the transmitted light images. As smaller features defined by their boundary cell walls, the visibility of the area of metaxylem lumen and the aerenchyma lacunae will be more affected by wall fluorescence than in the total root or stele areas, or object counts. This artefact is common to all fluorescence-based approaches, where the spread of light detected by the imaging system is spread wider than the point emitting the light (point spread function). In the RAT platform, these artefacts can be exacerbated by suboptimal sample orientation where fluorescence of the side walls might make measurement of the lumens or lacunae more challenging, so correct sample positioning is of importance, guidance for which is in the supplementary material('S7: Imaging Troubleshooting').

When contrasted against state of the art imaging equipment used for plant anatomical phenotyping, the RAT platform has several advantages (**Figure 4**) [1,40,62,63]. These are predominantly that it is cheap to set up and operate, and can achieve very high throughputs (Figure 4). Ultimately, it does have an operating cost (other than electricity) in the use of razor blades, where other systems (LAT) may just require power to operate, but this cost is close to negligible and relatively more than offset by the cost of maintenance of the more costly equipment. We feel the resolution is sufficient for anatomical trait quantification of most axial roots and larger lateral roots as well as several other tissues, but for imaging of especially small samples and those lacking secondary thickening, or subcellular detail, other techniques such as electron microscopy (SEM) or confocal laser scanning microscopy (CSLM) may be necessary [28,36,64]. Our optimisation of this platform for low cost and throughput in acquisition of 2D anatomical images comes at the cost of versatility. Confocal laser scanning microscopy (CLSM) and light sheet fluorescence microscopy (LSFM) both have the capacity to be used for 2D as well as 3D imaging, as well as quantitative imaging of fluorescence for detection of specific compounds and fluorescent proteins [65]. These, as well as X-ray microCT are non-destructive, and so can be used for 4D anatomical imaging in time series [66]. LAT imaging has potential to be developed further; validation of LAT images with other analysis approaches shows that fluorescence patterns in LAT images can be related to cell wall composition [34]. The use of LAT for sample surface preparation also means impermeable or hard to cut samples that would be challenging to prepare for CLSM can be imaged easily in both two and three dimensions.

Ultimately though, for our intended purpose of 2D anatomical data collection, our platform provides high throughput, with little to no sample preparation needed, and at a small fraction of the cost of other platforms often employed in anatomical studies (less than four thousand euros compared to tens or hundreds of thousand euros).

Root anatomical differences in variation along root axis

Leveraging RAT to investigate inter- and intra-specific variation in wheat roots, we discovered many root anatomical traits were significantly different between the historic and modern wheat cultivars surveyed. These differences became more frequent and more statistically pronounced when comparing positions on the root further along the root axis from the basal region. The anatomical differences along the root axis in the modern cultivar Tommi are most strongly observed in the vascular traits, the stele (-52.6 %) and metaxylem total (-40.7 %) areas, more so than the cortex area (-27.8 %). Similarly, in the older variety S. Dickkopf, the relative changes in root anatomy along the root axis were more strongly observed in stele (-30.3 %), and metaxylem total (-29.8 %) area than in the cortex (-13.4 %, non-significant) area. Comparing the differences in the

root composition ratios between sampling positions and cultivar makes these differences especially clear. Using this integrated metric accounting for metaxylem, cortex, and stele area as a proportion of the total root area (XCS) we can see that the root anatomy of the modern cultivar is not just changing along the length of the root but changing its proportional area by tissue type allometrically. This transition to a different root anatomical tissue composition appears driven by the vasculature in these instances. While there are also differences in the percentage change in area between positions in S. Dickkopf, they are less stark than in the modern cultivar, do not represent a significant change in XCS ratio, and therefore can be viewed as more isometric than allometric in nature. These results are interesting to note within the context of the broader root physiological results from the trial that yielded these samples [44]. In this study, it was seen that axial root number significantly decreased from the historic to the modern cultivar, and that measured and simulated whole root system hydraulic conductance also followed this trajectory. Interesting to note too is that in the root system analysis, there was no significant effect of breeding (cultivar release date) on crown root diameter [44]. This is reflected in our anatomical analysis, though the significant differences we observe in the vasculature between the historic and modern cultivar may well contribute to the described difference in root system hydraulic conductance. This highlights the importance of anatomical studies and the accessibility of tools to investigate anatomy in gaining a more complete and integrated understanding of the relationship between root physiology and hydraulic activity.

In the emerging field of high throughput root comparative anatomy, we consider the distinction between isometric changes and allometric transitions along the root axis to be a relatively underexplored phenomenon, potentially in part due to the lack of accessible sufficiently high throughput techniques for root anatomical imaging. While anatomical changes along individual axial roots have been shown to occur in a range of species, such as wheat [16,45,67–70], rice [67], millet [71], maize [39,72], wheatgrass, and alfalfa [73]. What drives these changes along the root also bears considering; while not mechanistically investigated, it is suggested that these are likely to relate to changes in Indole-3-acetic acid (IAA) gradient due to increasing distance from young leaves [68]. Additionally, plastic anatomical changes along individual roots have been shown to be affected by environmental factors such as hypoxia and compaction [47]. Whether these hormonal signals and or environmental factors dictate whether or not these changes occur, or the functional implications, rate, and position of these changes remains to be explored.

These findings demonstrate the efficacy of our platform; that the image quality is sufficient to observe and quantify variation in key functional traits, and that these images can be captured in sufficient throughput that it is feasible as well as beneficial to expand the scope of conventional sampling strategies for anatomical phenotyping. Relative to many other hardware requirements to achieve comparable image quality and speed (for specifically 2D anatomical phenotyping), our platform is cheap to purchase the components for, and run, representing good value for money, and easy to set up and operate.

Scope for future improvements

While the RAT platform is deliberately optimized for high-throughput phenotyping, it is important to acknowledge its inherent limitations and practical trade-offs. The image resolution is constrained by the consumer-grade optics, which may limit the detection of finer histological details such as the Casparian strip. Furthermore, the reliance on autofluorescence means that image quality can vary depending on the root's developmental stage, genotype, or environmental conditions. The manual cut through the sample, though effective, may lack the consistency of mechanical or vibratome slicing, which would be preferable for studies requiring the highest precision. Finally, while the mechanical clamp provides essential stability for imaging, it can cause compression

damage to the limited portion of the root tissue held within it. Beyond these hardware and methodological constraints, the speed of the workflow introduces important considerations for sample handling. Storing root samples in ~50% ethanol solution is a double-edged sword; while it prevents microbial decay and clears tissue to improve image contrast, it also makes the samples more prone to drying and cellular collapse upon removal from the preservative. This necessitates rapid imaging to avoid artifacts. Conversely, using lower ethanol concentrations to reduce evaporation can, due to the clamping pressure, result in a guttation effect that floods the cut surface and obscures cellular detail. While alternative preparation methods like critical point drying could potentially solve this, they would significantly increase preparation time and sample brittleness, undermining the platform's primary advantage of speed. Our platform has little to no sample preparation, optimising throughput in one way, however each sample must be processed individually as a result. An alternative is to prepare a large matrix of samples for sectioning and imaging in a single batch, as used in the recently developed 'AnatomyArray' [74]. This newly developed system uses a custom designed device for multiplexed root paraffin embedding and sectioning with a high speed and resolution imaging system. Combined with a complementary deep-learning image analysis tool, this system also offers a high-throughput root image analysis solution, using a very different sample preparation and imaging strategy to our 'one by one' RAT platform approach.

Despite these limitations, the platform's flexibility in sample type and size enhances its value as an accessible tool for large-scale screening. Our use of computer-controlled motorized stages provides a high degree of precision for tasks like focus stacking, but these are not essential. The core benefits of the platform can be achieved with more affordable, manually adjusted stages, including many open-source designs available for 3D printing. Looking forward, there are several clear avenues for improvement. The platform could be upgraded with higher-resolution imaging modules, integrated with automated sectioning systems to boost consistency, or coupled with real-time trait extraction using machine learning approaches. Currently image analysis is a rate limiting step in most anatomical phenotyping systems. Recently, significant advances have been made in the field of automated plant root anatomical image analysis through employing deep-learning approaches to develop networks that can segment and annotate root anatomical images for high throughput image analysis. These include systems such as AnatomyNet [74], DL-RootAnatomy [75], RootScan [71], RootAnalyzer [76], to name a few. These approaches greatly enhance throughput of image analysis pipelines, but transfer of these pipelines between species and imaging system can be challenging in the short term. Measuring these images with polygon selections that can be saved and efficiently exported for each image set has the added potential benefit of enabling translation of image measurements to training data for development of automated image analysis systems, suitable for images captured using the RAT platform. Developing an automated image analysis tool for images obtained using the RAT platform will further improve throughput, as well as reduce bias and inter-user variability at the image analysis step.

In summary, our UV autofluorescence imaging platform, even with its trade-offs, offers an accessible and scalable solution that facilitates the broader adoption of belowground trait analysis in root research and plant breeding.

Conclusions

This research yielded two key outcomes: a more accessible platform for rapid root anatomical phenotyping using nUV autofluorescence and blockface imaging, and a new understanding of intra-root anatomical variation. This study successfully developed and validated the Rapid Anatomics

Tool (RAT), a low-cost, high-throughput platform that makes detailed root anatomical analysis accessible to a broader range of researchers. With this platform, we have provided evidence that significant, allometric anatomical variation exists not only between wheat cultivars but also along the length of a single root. This work underscores the critical importance of strategic, multi-position sampling in root biology and provides the research community with an effective tool to explore the 'hidden half' in greater detail, accelerating our efforts to develop more resilient and efficient crops. This development and democratization of advanced imaging and analysis pipelines will be revolutionizing the field. This leap forward will finally enable the broader scientific community to systematically link genes to the anatomical phenotypes that drive physiological outcomes.

ACKNOWLEDGMENTS

General: Thanks to Annegret Wolf, Petra Linow, and Corinna Trautewig for their feedback on RAT design and usability

Author contributions: The system was conceived by H.M.S. and M.T.H. and developed by D.H.J. with input from H.M.S, J.S., D.M.W, J.A.A., and M.T.H., wheat trial growth, sampling, and management was carried out by J.B.C., D.B., and G.L., Cross platform comparison was carried out by J.S., M.S. created material for user guides and tested python scripts for camera control, testing and generation of images was done by J.S., M.T.H.,M.S., and D.H.J., writing of the manuscript was led by D.H.J., all authors contributed to writing, editing, and approved the manuscript.

Funding: Funded by the European Union (ERC, 101162856, FATE). Views and opinions are expressed are however those of the author(s) only and do not necessarily reflect those of the European Union or the European Research Council. Neither the European Union nor the granting authority can be held responsible for them. This study was funded by the Grains Research and Development Corporation 'Root structure and function traits: Overcoming the root phenotyping bottleneck in cereals' project (DHJ). JCBC is funded by Deutsche Forschungsgemeinschaft (DFG, German Research Foundation) (SFB 1502/1-2022, Projektnummer: 450058266). Additional funding for this work was provided by the New Roots for Restoration Biology Integration Institute (NSF 2120153) and by the Miller Lab at the Donald Danforth Plant Science Center. G.L. is co-funded by the European Union (ERC grant 101125638), J.F.S. is funded by a National Science Foundation Postdoctoral Research Fellowship in Biology (IOS-2305703).

Competing interests: The author(s) declare(s) that there is no conflict of interest regarding the publication of this article.

DATA AVAILABILITY

3D design files (STL) are provided in the supplementary material. The Python script used to control image acquisition using the specific USB microscope used in this study is available in the supplementary materials, though requires drivers from the software development kit from the manufacturer. Datasets generated and analysed are available from the corresponding authors on reasonable request.

SUPPLEMENTARY MATERIALS

Supplementary Material: ‘RAT_Base_plate(DinoLite_manual_stage).stl’

Supplementary Material: ‘RAT_Base_plate(motorized_stage).stl’

Supplementary Material: ‘RAT_Lid_X.stl’

Supplementary Material: ‘RAT_DinoLite_Custom_Workflow_Controller.py’

Supplementary Material: ‘User_guide.docx’

Supplementary Material: ‘Cross-platform_comparison.docx’

REFERENCES

[1] C.F. Strock, H.M. Schneider, J.P. Lynch, Anatomics: High-throughput phenotyping of plant anatomy, Trends in Plant Science 27 (2022) 520–523. https://doi.org/10.1016/j.tplants.2022.02.009.

[2] J.C. Baca Cabrera, J. Vanderborght, V. Couvreur, D. Behrend, T. Gaiser, T.H. Nguyen, G. Lobet, Root hydraulic properties: An exploration of their variability across scales, Plant Direct 8 (2024) e582. https://doi.org/10.1002/pld3.582.

[3] Y. Boursiac, C. Pradal, F. Bauget, M. Lucas, S. Delivorias, C. Godin, C. Maurel, Phenotyping and modeling of root hydraulic architecture reveal critical determinants of axial water transport, Plant Physiology 190 (2022) 1289–1306. https://doi.org/10.1093/plphys/kiac281.

[4] H. Bramley, N.C. Turner, D.W. Turner, S.D. Tyerman, Roles of Morphology, Anatomy, and Aquaporins in Determining Contrasting Hydraulic Behavior of Roots, Plant Physiology 150 (2009) 348–364. https://doi.org/10.1104/pp.108.134098.

[5] J.P. Lynch, C.F. Strock, H.M. Schneider, J.S. Sidhu, I. Ajmera, T. Galindo-Castañeda, S.P. Klein, M.T. Hanlon, Root anatomy and soil resource capture, Plant Soil 466 (2021) 21–63. https://doi.org/10.1007/s11104-021-05010-y.

[6] J.P. Lynch, Root phenes that reduce the metabolic costs of soil exploration: opportunities for 21st century agriculture, Plant, Cell & Environment 38 (2015) 1775–1784. https://doi.org/10.1111/pce.12451.

[7] J.S. Sidhu, I. Lopez-Valdivia, C.F. Strock, H.M. Schneider, J.P. Lynch, Cortical parenchyma wall width regulates root metabolic cost and maize performance under suboptimal water availability, Journal of Experimental Botany 75 (2024) 5750–5767. https://doi.org/10.1093/jxb/erae191.

[8] T. Galindo-Castañeda, J.P. Lynch, J. Six, M. Hartmann, Improving Soil Resource Uptake by Plants Through Capitalizing on Synergies Between Root Architecture and Anatomy and Root-Associated Microorganisms, Front. Plant Sci. 13 (2022). https://doi.org/10.3389/fpls.2022.827369.

[9] H.W.G. Birt, C.L. Tharp, G.F. Custer, F. Dini-Andreote, Root phenotypes as modulators of microbial microhabitats, Front. Plant Sci. 13 (2022). https://doi.org/10.3389/fpls.2022.1003868.

[10] T. Yamauchi, O. Pedersen, M. Nakazono, N. Tsutsumi, Key root traits of Poaceae for adaptation to soil water gradients, New Phytologist 229 (2021) 3133–3140. https://doi.org/10.1111/nph.17093.

[11] D.H. Jones, K. Kajala, D. Kawa, I. Lopez-Valdivia, T. Kreszies, H.M. Schneider, The root cortex of the Poaceae: a diverse, dynamic, and dispensable tissue, Plant Soil (2025). https://doi.org/10.1007/s11104-025-07498-0.

[12] H.M. Schneider, S.P. Klein, M.T. Hanlon, S. Kaeppler, K.M. Brown, J.P. Lynch, Genetic control of root anatomical plasticity in maize, The Plant Genome 13 (2020) e20003. https://doi.org/10.1002/tpg2.20003.

[13] F. Hochholdinger, P. Yu, C. Marcon, Genetic Control of Root System Development in Maize, Trends in Plant Science 23 (2018) 79–88. https://doi.org/10.1016/j.tplants.2017.10.004.

[14] R. Fusi, S.G. Milner, S. Rosignoli, R. Bovina, C. De Jesus Vieira Teixeira, H. Lou, B.S. Atkinson, A.N. Borkar, L.M. York, D.H. Jones, C.J. Sturrock, N. Stein, M. Mascher, R. Tuberosa, D. O’Connor, M.J. Bennett, A. Bishopp, S. Salvi, R. Bhosale, The auxin efflux carrier PIN1a regulates vascular patterning in cereal roots, New Phytologist 244 (2024) 104–115. https://doi.org/10.1111/nph.19777.

[15] J.E. Reeger, M. Wheatley, Y. Yang, K.M. Brown, Targeted mutation of transcription factor genes alters metaxylem vessel size and number in rice roots, Plant Direct 5 (2021) e00328. https://doi.org/10.1002/pld3.328.

[16] N.N. Kadam, A. Tamilselvan, L.M.F. Lawas, C. Quinones, R.N. Bahuguna, M.J. Thomson, M. Dingkuhn, R. Muthurajan, P.C. Struik, X. Yin, S.V.K. Jagadish, Genetic Control of Plasticity in Root Morphology and

Anatomy of Rice in Response to Water Deficit, Plant Physiology 174 (2017) 2302–2315. https://doi.org/10.1104/pp.17.00500.
[17] R.A. Richards, J.B. Passioura, A breeding program to reduce the diameter of the major xylem vessel in the seminal roots of wheat and its effect on grain yield in rain-fed environments, Aust. J. Agric. Res. 40 (1989) 943–950. https://doi.org/10.1071/ar9890943.
[18] L. Comas, S. Becker, V.M.V. Cruz, P.F. Byrne, D.A. Dierig, Root traits contributing to plant productivity under drought, Front. Plant Sci. 4 (2013). https://doi.org/10.3389/fpls.2013.00442.
[19] M.C. Drew, C.-J. He, P.W. Morgan, Decreased Ethylene Biosynthesis, and Induction of Aerenchyma, by Nitrogen- or Phosphate-Starvation in Adventitious Roots of Zea mays L. 1, Plant Physiology 91 (1989) 266–271. https://doi.org/10.1104/pp.91.1.266.
[20] P. Saengwilai, E.A. Nord, J.G. Chimungu, K.M. Brown, J.P. Lynch, Root Cortical Aerenchyma Enhances Nitrogen Acquisition from Low-Nitrogen Soils in Maize, Plant Physiology 166 (2014) 726–735. https://doi.org/10.1104/pp.114.241711.
[21] J.A. Postma, A. Dathe, J.P. Lynch, The Optimal Lateral Root Branching Density for Maize Depends on Nitrogen and Phosphorus Availability, Plant Physiology 166 (2014) 590–602. https://doi.org/10.1104/pp.113.233916.
[22] T. Galindo-Castañeda, K.M. Brown, J.P. Lynch, Reduced root cortical burden improves growth and grain yield under low phosphorus availability in maize, Plant Cell Environ 41 (2018) 1579–1592. https://doi.org/10.1111/pce.13197.
[23] J.G. Chimungu, K.M. Brown, J.P. Lynch, Reduced Root Cortical Cell File Number Improves Drought Tolerance in Maize, Plant Physiology 166 (2014) 1943–1955. https://doi.org/10.1104/pp.114.249037.
[24] N. Grew, The anatomy of vegetables begun, (1672). https://library.si.edu/digital-library/book/anatomyofvegetab00grew (accessed July 13, 2025).
[25] N. Grew, The Anatomy of Plants, 1st ed., W. Rawlins, London, 1682. https://www.loc.gov/item/06006649/.
[26] A. Arber, Monocotyledons: A Morphological Study, Cambridge University Press, Cambridge, 1925. https://doi.org/10.1017/CBO9780511708626.
[27] K. Esau, Plant anatomy, New York ; London : Wiley, 1965. http://archive.org/details/plantanatomy00esau_0 (accessed February 26, 2025).
[28] M. Watt, L.J. Magee, M.E. McCully, Types, structure and potential for axial water flow in the deepest roots of field-grown cereals, New Phytologist 178 (2008) 135–146. https://doi.org/10.1111/j.1469-8137.2007.02358.x.
[29] J. Hughes, M.E. McCully, The Use of an Optical Brightener in the Study of Plant Structure, Stain Technology 50 (1975) 319–329. https://doi.org/10.3109/10520297509117082.
[30] D.C. Hoppe, M.E. McCully, C.L. Wenzel, The nodal roots of Zea: their development in relation to structural features of the stem, Can. J. Bot. 64 (1986) 2524–2537. https://doi.org/10.1139/b86-335.
[31] T.P. O'Brien, N. Feder, M.E. McCully, Polychromatic staining of plant cell walls by toluidine blue O, Protoplasma 59 (1964) 368–373. https://doi.org/10.1007/BF01248568.
[32] I. Karas, M.E. McCully, Further studies of the histology of lateral root development inZea mays, Protoplasma 77 (1973) 243–269. https://doi.org/10.1007/BF01276762.
[33] H.M. Schneider, Characterization, costs, cues and future perspectives of phenotypic plasticity, Ann Bot 130 (2022) 131–148. https://doi.org/10.1093/aob/mcac087.
[34] H.M. Schneider, C.F. Strock, M.T. Hanlon, D.J. Vanhees, A.C. Perkins, I.B. Ajmera, J.S. Sidhu, S.J. Mooney, K.M. Brown, J.P. Lynch, Multiseriate cortical sclerenchyma enhance root penetration in compacted soils, Proceedings of the National Academy of Sciences 118 (2021) e2012087118. https://doi.org/10.1073/pnas.2012087118.
[35] P.-F. Li, B.-L. Ma, X.-F. Wei, S. Guo, Y.-Q. Ma, Deeper root distribution and optimized root anatomy help improve dryland wheat yield and water use efficiency under low water conditions, Plant Soil 501 (2024) 437–454. https://doi.org/10.1007/s11104-024-06526-9.
[36] A. Ware, D.H. Jones, P. Flis, E. Chrysanthou, K.E. Smith, B.M.C. Kümpers, L. Yant, J.A. Atkinson, D.M. Wells, R. Bhosale, A. Bishopp, Loss of ancestral function in duckweed roots is accompanied by progressive anatomical reduction and a re-distribution of nutrient transporters, Current Biology 33 (2023) 1795-1802.e4. https://doi.org/10.1016/j.cub.2023.03.025.
[37] J.A. Atkinson, M.P. Pound, M.J. Bennett, D.M. Wells, Uncovering the hidden half of plants using new advances in root phenotyping, Current Opinion in Biotechnology 55 (2019) 1–8. https://doi.org/10.1016/j.copbio.2018.06.002.
[38] J.P. Lynch, Roots of the Second Green Revolution, Aust. J. Bot. 55 (2007) 493–512. https://doi.org/10.1071/BT06118.
[39] A. Heymans, V. Couvreur, G. Lobet, Combining cross-section images and modeling tools to create high-resolution root system hydraulic atlases in Zea mays, Plant Direct 5 (2021) e00290. https://doi.org/10.1002/pld3.334.

[40] D.J. Thomas, J. Rainbow, L.E. Bartley, The rapid-tome, a 3D-printed microtome, and an updated hand-sectioning method for high-quality plant sectioning, Plant Methods 19 (2023) 12. https://doi.org/10.1186/s13007-023-00986-3.
[41] J.A. Atkinson, D.M. Wells, An Updated Protocol for High Throughput Plant Tissue Sectioning, Front. Plant Sci. 8 (2017). https://doi.org/10.3389/fpls.2017.01721.
[42] I.L. Cunha Neto, B.T. Hall, A.R. Lanba, J.D. Blosenski, J.G. Onyenedum, Laser ablation tomography (LATscan) as a new tool for anatomical studies of woody plants, New Phytologist 239 (2023) 429–444. https://doi.org/10.1111/nph.18831.
[43] H.M. Schneider, C.F. Strock, M.T. Hanlon, D.J. Vanhees, A.C. Perkins, I.B. Ajmera, J.S. Sidhu, S.J. Mooney, K.M. Brown, J.P. Lynch, Multiseriate cortical sclerenchyma enhance root penetration in compacted soils, Proc Natl Acad Sci U S A 118 (2021) e2012087118. https://doi.org/10.1073/pnas.2012087118.
[44] J.C. Baca Cabrera, J. Vanderborght, Y. Boursiac, D. Behrend, T. Gaiser, T.H. Nguyen, G. Lobet, Decreased root hydraulic traits in German winter wheat cultivars over 100 years of breeding, Plant Physiology 198 (2025) kiaf166. https://doi.org/10.1093/plphys/kiaf166.
[45] N.N. Kadam, X. Yin, P.S. Bindraban, P.C. Struik, K.S.V. Jagadish, Does Morphological and Anatomical Plasticity during the Vegetative Stage Make Wheat More Tolerant of Water Deficit Stress Than Rice?, Plant Physiology 167 (2015) 1389–1401. https://doi.org/10.1104/pp.114.253328.
[46] P. Yu, P.J. White, F. Hochholdinger, C. Li, Phenotypic plasticity of the maize root system in response to heterogeneous nitrogen availability, Planta 240 (2014) 667–678. https://doi.org/10.1007/s00425-014-2150-y.
[47] H. Sjulgård, D. Iseskog, N. Kirchgessner, A.G. Bengough, T. Keller, T. Colombi, Reversible and irreversible root phenotypic plasticity under fluctuating soil physical conditions, Environmental and Experimental Botany 188 (2021) 104494. https://doi.org/10.1016/j.envexpbot.2021.104494.
[48] M. Kittelmann, C. Hawes, L. Hughes, Serial block face scanning electron microscopy and the reconstruction of plant cell membrane systems, Journal of Microscopy 263 (2016) 200–211. https://doi.org/10.1111/jmi.12424.
[49] L. Donaldson, Autofluorescence in Plants, Molecules 25 (2020) 2393. https://doi.org/10.3390/molecules25102393.
[50] A. Alony, R. Linker, Development of a laser-induced fluorescence imaging system for root activity and rhizosphere visualisation, Biosystems Engineering 114 (2013) 466–473. https://doi.org/10.1016/j.biosystemseng.2012.08.006.
[51] A. Wasson, L. Bischof, A. Zwart, M. Watt, A portable fluorescence spectroscopy imaging system for automated root phenotyping in soil cores in the field, Journal of Experimental Botany 67 (2016) 1033–1043. https://doi.org/10.1093/jxb/erv570.
[52] M. Corcel, M.-F. Devaux, F. Guillon, C. Barron, Comparison of UV and visible autofluorescence of wheat grain tissues in macroscopic images of cross-sections and particles, Computers and Electronics in Agriculture 127 (2016) 281–288. https://doi.org/10.1016/j.compag.2016.06.016.
[53] T.J. Pegg, D.K. Gladish, R.L. Baker, Algae to angiosperms: Autofluorescence for rapid visualization of plant anatomy among diverse taxa, Applications in Plant Sciences 9 (2021) e11437. https://doi.org/10.1002/aps3.11437.
[54] D. Behrend, T. Nguyen, H. Hüging, J.B. Cabrera, G. Lobet, S. Seidel, A. Srivastava, C.G. Bazzo, N. Kramer, P. Nachtweide, J. Vanderborght, F. Ewert, T. Gaiser, Biomass partitioning and canopy architecture of six German winter wheat cultivars released between 1895 and 2002, (2025). https://www.authorea.com/users/960946/articles/1329726-biomass-partitioning-and-canopy-architecture-of-six-german-winter-wheat-cultivars-released-between-1895-and-2002?commit=4a9a6edf6e96aea9db67004fd6725c3fccc57971 (accessed October 28, 2025).
[55] D. Vetterlein, T. Kühn, K. Kaiser, R. Jahn, Illite transformation and potassium release upon changes in composition of the rhizophere soil solution, Plant Soil 371 (2013) 267–279. https://doi.org/10.1007/s11104-013-1680-6.
[56] S.J. Seidel, T. Gaiser, H.E. Ahrends, H. Hüging, S. Siebert, S.L. Bauke, M.I. Gocke, M. Koch, K. Schweitzer, G. Schaaf, F. Ewert, Crop response to P fertilizer omission under a changing climate - Experimental and modeling results over 115 years of a long-term fertilizer experiment, Field Crops Research 268 (2021) 108174. https://doi.org/10.1016/j.fcr.2021.108174.
[57] H.E. Ahrends, W. Eugster, T. Gaiser, V. Rueda-Ayala, H. Hüging, F. Ewert, S. Siebert, Genetic yield gains of winter wheat in Germany over more than 100 years (1895–2007) under contrasting fertilizer applications, Environ. Res. Lett. 13 (2018) 104003. https://doi.org/10.1088/1748-9326/aade12.
[58] I.M. Hernández-Ochoa, T. Gaiser, H. Hüging, F. Ewert, Yield components and yield quality of old and modern wheat cultivars as affected by cultivar release date, N fertilization and environment in Germany, Field Crops Research 302 (2023) 109094. https://doi.org/10.1016/j.fcr.2023.109094.
[59] V. Rueda-Ayala, H.E. Ahrends, S. Siebert, T. Gaiser, H. Hüging, F. Ewert, Impact of nutrient supply on the expression of genetic improvements of cereals and row crops – A case study using data from a long-term

fertilization experiment in Germany, European Journal of Agronomy 96 (2018) 34–46. https://doi.org/10.1016/j.eja.2018.03.002.

[60] L.M. York, Phenotyping Crop Root Crowns: General Guidance and Specific Protocols for Maize, Wheat, and Soybean, in: D. Ristova, E. Barbez (Eds.), Root Development: Methods and Protocols, Springer, New York, NY, 2018: pp. 23–32. https://doi.org/10.1007/978-1-4939-7747-5_2.

[61] J. Schindelin, I. Arganda-Carreras, E. Frise, V. Kaynig, M. Longair, T. Pietzsch, S. Preibisch, C. Rueden, S. Saalfeld, B. Schmid, J.-Y. Tinevez, D.J. White, V. Hartenstein, K. Eliceiri, P. Tomancak, A. Cardona, Fiji: an open-source platform for biological-image analysis, Nat Methods 9 (2012) 676–682. https://doi.org/10.1038/nmeth.2019.

[62] F.E. Gomez, G. Carvalho, F. Shi, A.H. Muliana, W.L. Rooney, High throughput phenotyping of morpho-anatomical stem properties using X-ray computed tomography in sorghum, Plant Methods 14 (2018) 59. https://doi.org/10.1186/s13007-018-0326-3.

[63] D. von Wangenheim, R. Hauschild, J. Friml, Light Sheet Fluorescence Microscopy of Plant Roots Growing on the Surface of a Gel, Journal of Visualized Experiments (JoVE) (2017) e55044. https://doi.org/10.3791/55044.

[64] P.J. DART, Scanning Electron Microscopy of Plant Roots, Journal of Experimental Botany 22 (1971) 163–168. https://doi.org/10.1093/jxb/22.1.163.

[65] S. Henry, F. Divol, M. Bettembourg, C. Bureau, E. Guiderdoni, C. Périn, A. Diévart, Immunoprofiling of Rice Root Cortex Reveals Two Cortical Subdomains, Front. Plant Sci. 6 (2016). https://doi.org/10.3389/fpls.2015.01139.

[66] S. Teramoto, Y. Uga, Four-dimensional measurement of root system development using time-series three-dimensional volumetric data analysis by backward prediction, Plant Methods 18 (2022) 133. https://doi.org/10.1186/s13007-022-00968-x.

[67] W. Ouyang, X. Yin, J. Yang, P.C. Struik, Comparisons with wheat reveal root anatomical and histochemical constraints of rice under water-deficit stress, Plant Soil 452 (2020) 547–568. https://doi.org/10.1007/s11104-020-04581-6.

[68] H. Wu, M. Jaeger, M. Wang, B. Li, B.G. Zhang, Three-dimensional distribution of vessels, passage cells and lateral roots along the root axis of winter wheat (Triticum aestivum), Annals of Botany 107 (2011) 843–853. https://doi.org/10.1093/aob/mcr005.

[69] S. Sharma, D.A. DeMason, B. Ehdaie, A.J. Lukaszewski, J.G. Waines, Dosage effect of the short arm of chromosome 1 of rye on root morphology and anatomy in bread wheat, Journal of Experimental Botany 61 (2010) 2623–2633. https://doi.org/10.1093/jxb/erq097.

[70] B.L. Harrison Day, K.M. Johnson, V. Tonet, I. Bourbia, C. Blackman, T.J. Brodribb, The root of the problem: diverse vulnerability to xylem cavitation found within the root system of wheat plants, New Phytologist 239 (2023) 1239–1252. https://doi.org/10.1111/nph.19017.

[71] P. Affortit, A. Faye, D.H. Jones, E. Benson, B. Sine, J. Burridge, M.S. Ndoye, L. Barry, D. Moukouanga, S. Barnard, R. Bhosale, T. Pridmore, P. Gantet, V. Vadez, P. Cubry, N. Kane, M. Bennett, J.A. Atkinson, L. Laplaze, D.M. Wells, A. Grondin, Root metaxylem area influences drought tolerance and transpiration in pearl millet in a soil texture dependent manner, (2024) 2024.11.09.622826. https://doi.org/10.1101/2024.11.09.622826.

[72] L.V. Kozlova, A.R. Nazipova, O.V. Gorshkov, A.A. Petrova, T.A. Gorshkova, Elongating maize root: zone-specific combinations of polysaccharides from type I and type II primary cell walls, Sci Rep 10 (2020) 10956. https://doi.org/10.1038/s41598-020-67782-0.

[73] C. Clément, H.M. Schneider, D.B. Dresbøll, J.P. Lynch, K. Thorup-Kristensen, Root and xylem anatomy varies with root length, root order, soil depth and environment in intermediate wheatgrass (Kernza®) and alfalfa, Annals of Botany 130 (2022) 367–382. https://doi.org/10.1093/aob/mcac058.

[74] Y. Cheng, J. Shi, Z. Pang, N. Xu, K. Chai, J. Gao, Z. Jia, B. Hao, H. Yin, R. Fang, S. Xie, W. Chen, D. Xiang, Z. Zhou, W. Yang, Q. Li, AnatomyArray: A high-throughput platform for anatomical phenotyping in plants, Plant Cell 37 (2025) koaf223. https://doi.org/10.1093/plcell/koaf223.

[75] C. Wang, X. Li, D. Caragea, R. Bheemanahallia, S.V.K. Jagadish, Root anatomy based on root cross-section image analysis with deep learning, Computers and Electronics in Agriculture 175 (2020) 105549. https://doi.org/10.1016/j.compag.2020.105549.

[76] J. Chopin, H. Laga, C.Y. Huang, S. Heuer, S.J. Miklavcic, RootAnalyzer: A Cross-Section Image Analysis Tool for Automated Characterization of Root Cells and Tissues, PLOS ONE 10 (2015) e0137655. https://doi.org/10.1371/journal.pone.0137655.

Declaration of Interest Statement

☒ The authors declare that they have no known competing financial interests or personal relationships that could have appeared to influence the work reported in this paper.

☐ The author is an Editorial Board Member/Editor-in-Chief/Associate Editor/Guest Editor for this journal and was not involved in the editorial review or the decision to publish this article.

☐ The authors declare the following financial interests/personal relationships which may be considered as potential competing interests: